H^∞ Control Applied to Boost Power Converters

Rami Naim, George Weiss, and Shmuel (Sam) Ben-Yaakov

Abstract—**The controller in a pulse-width-modulation (PWM) power converter has to stabilize the system and guarantee an almost constant output voltage in spite of the perturbations in the input voltage and output load over as large a bandwidth as possible. Boost and flyback converters have a right-half-plane zero (RHPZ) in their transfer function from the duty cycle to the output voltage, which makes it difficult to achieve the aforementioned goals. We propose to design the controller using H^∞ control theory, via the solution of two algebraic Riccati equations. The almost optimal H^∞ controller is of the same order as the converter and has a relatively low dc gain. The closed-loop characteristics of a typical low-power boost converter with four different control schemes were compared by computer simulation. The H^∞ control was found to be superior in a wide frequency range, while being outperformed by the others at extremely low frequencies. Good agreement was found between simulation results and experimental measurements.**

Index Terms—**Boost converter, current-mode control, H^∞ control, Riccati equation.**

I. Introduction

PULSE-WIDTH-modulation (PWM) dc–dc converters are nonlinear and time-variant systems. After linearization of the average model (see, e.g., Sum [10]), we obtain a linear time-invariant model that describes approximately the behavior of the system for frequencies up to half of the switching frequency. The tasks of the controller in dc–dc switch-mode systems (aside from the fundamental requirement of small static or dc error) are to:

1) assure stability of the closed-loop system;
2) minimize sensitivity to load changes, i.e., reduce the output impedance;
3) attenuate input–output transmission (low audiosusceptibility).

In addition, an underlining requirement of the controller design is to maintain characteristics 2) and 3) over as large a bandwidth as possible. Traditional designs of feedback loops in dc–dc switch-mode systems are based on frequency-domain analysis (after linearization). A major problem is encountered, however, when the transfer function of the power stage (from the control input to the output voltage) has a right-half-plane zero (RHPZ). In such cases (e.g., boost or flyback converters), the presence of the RHPZ severely restricts the closed-loop bandwidth that can be obtained by the classical frequency-domain approach, see, e.g., Pressman [8] or Dixon [2].

The recently introduced H^∞ control strategy (see, e.g., Doyle *et al.* [3], Francis [4], or Limebeer and Green [6]) opens up new possibilities for controlling switch-mode systems. One main difference between this control scheme and the traditional ones is in relation to the attainment of low-output impedance. In the conventional design, the low-output impedance is not a direct design goal. Rather, it is obtained indirectly by increasing the loop gain. However, this increase is normally in conflict with the phase-margin requirement. Consequently, the presence of an RHPZ severely restricts the closed-loop bandwidth that can be obtained. In the H^∞ control strategy, the control goals can be formulated to directly include the reduction of the output impedance as much as possible over a given frequency range. It would thus appear then that H^∞ control could overcome some of the difficulties encountered with the conventional control approach. The objectives of the controller match very well with the so-called standard problem dealt with in H^∞ control theory (see [3], [4], and [6]).

The suboptimal solution of the standard problem can be found via the description of the (linearized) system in state space and the solution of two algebraic Riccati equations, for which reliable programs are available in MATLAB (MathWorks, Inc.) through the Robust Control Toolbox created by Chiang and Safonov. The nearly optimal H^∞ controller is of the same order as the converter and has a relatively low dc gain (in contrast with the classical idea of using high gain at low frequencies), so it is easy to implement.

We have compared the closed-loop performance of a low-power boost converter with four different controllers, designed using the voltage-mode, feedforward, current-mode and H^∞ control methods. We have derived the control law for each control scheme and then compared the closed-loop characteristics by MATLAB Simulink and HSPICE (Meta Software, Inc.) simulations. The performance of the H^∞ controller has also been verified experimentally.

II. H^∞ Control: Some General Facts

The space RH^∞ consists of all real rational functions, which are bounded on the right-half plane. The natural norm on this vector space is the *supremum* of the absolute value

$$\|G\|_\infty = \sup_{\mathrm{Re}\, s>0} |G(s)| = \sup_{\omega\in\mathbb{R}} |G(i\omega)|. \qquad (1)$$

Note that $\|G\|_\infty$ is the maximal gain of G, if we think of G as a transfer function. If G is matrix valued, then we say that $G \in RH^\infty$ if each entry of G belongs to the space RH^∞. In

Manuscript received May 25, 1995; revised December 5, 1996. Recommended by Associate Editor, D. C. Hamill.

R. Naim is with the Hardware Department, Telrad Ltd., Lod, Israel.

G. Weiss is with the Center for Systems and Control Engineering, School of Engineering, University of Exeter, Exeter EX4 4QF, U.K.

S. Ben-Yaakov is with the Department of Electrical Engineering, Ben-Gurion University, Beer-Sheva 84105, Israel.

Publisher Item Identifier S 0885-8993(97)04978-8.

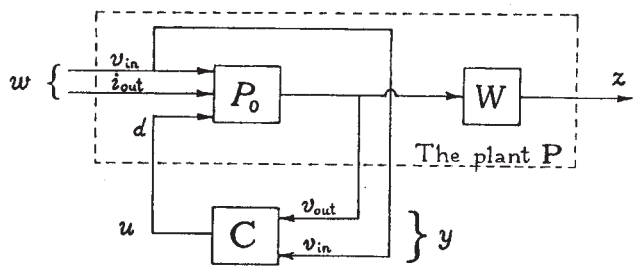

Fig. 1. The control of the converter as a standard H^∞ control problem.

this case, $\|G\|_\infty$ is defined as in (1), but absolute values have to be replaced by matrix norms (i.e., greatest singular values).

After linearization of the average model of a converter (see Sum [10]), we can translate the problem of designing a controller for this converter to the standard problem of H^∞ control, as illustrated in Fig. 1. In this figure and the subsequent text, lower case symbols like v_{in}, v_{out}, i_{out}, and d denote deviations of signals from their nominal values (which are denoted by capital letters).

In the diagram, P_0 is the converter, $\mathbf{C}$ is the controller to be designed, and W is a stable weight function. The vector w contains the perturbations (v_{in} and i_{out}), the output z is the weighted error signal, the vector y contains the measurement outputs of the plant (v_{out} and v_{in}), and the control input u is the duty cycle d. We denote by T_{zw} the transfer function from w to z (in closed loop, i.e., with the controller connected to the plant).

The standard problem of H^∞ control is to find a controller $\mathbf{C}$, which stabilizes the plant (i.e., the closed-loop system is stable) and also minimizes the H^∞ norm of T_{zw}. The weight function W expresses the relative importance of different frequencies (it is bigger for frequencies, where the presence of perturbations in the error signal is more disturbing). By adjusting the weight function, we can obtain, for example, better performance at lower frequencies at the expense of worse attenuation at higher frequencies and the other way around. Note that the components of T_{zw} are the input–output voltage-disturbance attenuation and the output impedance, both multiplied by the weight function W. Thus, our design objective includes minimization of the weighted output impedance.

The converter P_0 and weight function W can be combined to form the *plant* $\mathbf{P}$, which is a system with inputs w, u and outputs z, y. Note that there is no physical realization of W involved—W appears only in our computations.

We give a very brief description of the state-space solution of the standard problem for a general plant (not related to converters) following [6]. Assume that we can describe a plant $\mathbf{P}$ by equations of the form

$$\begin{aligned} \dot{x} &= Ax + B_1 w + B_2 u \\ z &= C_1 x + D_{11} w + D_{12} u \\ y &= C_2 x + D_{21} w + D_{22} u \end{aligned} \tag{2}$$

where $x(t) \in \mathbb{R}^n$ is the state, $u(t) \in \mathbb{R}^m$ is the control input, and $y(t) \in \mathbb{R}^p$ is the measurement output. The *standard problem* of H^∞ control is to find a controller $\mathbf{C}$ to be connected from y to u such that: 1) the resulting closed-loop system is stable and 2) the H^∞ norm of the transfer function from w to z is minimized. In practice, we are not really seeking the optimal solution, but a nearly optimal one, i.e., one for which the aforementioned H^∞ norm is close to being minimal.

For any positive integer k, I_k will denote the identity matrix of order k and D' will denote the transpose of the matrix D. We make the following assumptions about the plant $\mathbf{P}$:

$$\begin{aligned} D_{11} &= 0 \\ D_{22} &= 0 \end{aligned} \tag{3}$$

$$\begin{aligned} D_{12}' D_{12} &= I_m \\ D_{21} D_{21}' &= I_p \end{aligned} \tag{4}$$

$$(A,\ B_2,\ C_2) \text{ is stabilizable and detectable} \tag{5}$$

$$\operatorname{rank}\begin{bmatrix} j\omega I_n - A & B_2 \\ C_1 & D_{12} \end{bmatrix} = m + n, \qquad \text{for all real } \omega \tag{6}$$

$$\operatorname{rank}\begin{bmatrix} j\omega I_n - A & B_1 \\ C_2 & D_{21} \end{bmatrix} = p + n, \qquad \text{for all real } \omega. \tag{7}$$

Most plants $\mathbf{P}$ satisfy assumptions (5)–(7) (these are not restrictive), but do not satisfy assumptions (3) and (4). For plants satisfying (5)–(7) together with the (nonrestrictive) assumptions

$$\begin{aligned} \operatorname{rank} D_{12} &= m \\ \operatorname{rank} D_{21} &= p \end{aligned} \tag{8}$$

loop shifting and scaling procedures have been developed, see Safonov *et al.* [9] or Limebeer and Green [6, ch. 4]. These transformations enable us to reformulate the standard problem for the plant $\mathbf{P}$ as a standard problem for a modified plant $\hat{\mathbf{P}}$ such that $\hat{\mathbf{P}}$ satisfies all the assumptions (3)–(7).

We recall the concept of a stabilizing solution of a Riccati equation. Assume that three matrices A, Q, and R of dimension $n \times n$ are given, where Q and R are symmetric. The *Riccati equation* associated to A, Q, and R is

$$A'X + XA + XRX - Q = 0. \tag{9}$$

A matrix X is called a *stabilizing solution* of (9) if:

1) X is a solution of the Riccati equation;
2) X is symmetric;
3) $A + RX$ is stable.

The *Hamiltonian matrix* for the Riccati equation (9) is defined by

$$H = \begin{bmatrix} A & R \\ Q & -A' \end{bmatrix}.$$

Clearly, the Riccati equation is completely determined by this matrix. There is a stabilizing solution for the Riccati equation if and only if $(A,\ R)$ is stabilizable and the Hamiltonian H has no eigenvalues on the imaginary axis. In this case, this stabilizing solution is unique, and we denote it by $\operatorname{Ric}(H)$.

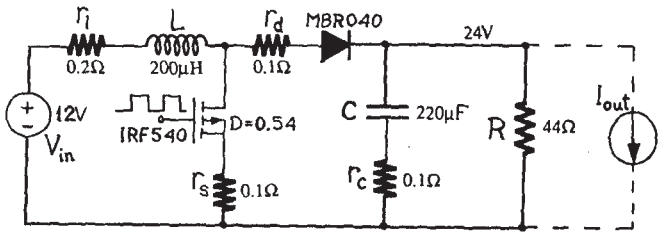

Fig. 2. The boost converter in the design example.

For the plant $\mathbf{P}$ satisfying the assumptions (3)–(7) and for any number $\gamma > 0$, we define two Hamiltonian matrices

$$M = \begin{bmatrix} A & \gamma^{-2}B_1B_1' - B_2B_2' \\ -C_1'C_1 & -A' \end{bmatrix}$$
$$J = \begin{bmatrix} A' & \gamma^{-2}C_1'C_1 - C_2'C_2 \\ -B_1B_1' & -A \end{bmatrix}.$$

We denote by T_{zw} the transfer function from w to z after a controller $\mathbf{C}$ has been connected to $\mathbf{P}$ from y to u.

Theorem: Let $\gamma > 0$. There is a stabilizing controller $\mathbf{C}$ for the plant $\mathbf{P}$ such that $\|T_{zw}\|_\infty < \gamma$ if and only if:

1) there is a stabilizing solution $X = \mathrm{Ric}(M)$;
2) there is a stabilizing solution $Y = \mathrm{Ric}(J)$;
3) $\rho(XY) < \gamma^2$ (ρ denotes the spectral radius).

Moreover, one of these stabilizing controllers $\mathbf{C}$ has a realization of the form

$$A_c = A + (\gamma^{-2}B_1B_1' - B_2B_2')X - B_2D_{12}'C_1$$
$$B_c = B_1D_{21}'$$
$$C_c = -D_{12}'C_1 + B_2'X$$
$$D_c = 0.$$

Let γ_{opt} be the *infimum* of those $\gamma > 0$ for which $\|T_{zw}\|_\infty < \gamma$ can be achieved. We can obtain a controller with $\|T_{zw}\|_\infty$ as close to γ_{opt} as we wish by an iterative search. The Robust Control Toolbox of MATLAB contains a function called *hinfopt*, which does this search, yielding a controller that is nearly optimal (in the H^∞ sense). This function needs only the state-space description of the plant (including the weight function), as in (2).

III. The Boost Converter

As a design example, we took a typical low-power boost converter operated in continuous conduction mode, shown in Fig. 2, which transforms a nominal 12-V input voltage into 24 V at its output. The switching frequency is 240 kHz. The role of the current source in the output is to simulate changes in the load (changes in the output current). The series resistance of the inductor, switch, diode, and capacitor are all shown.

The controller imposes the duty cycle D, which is the ratio between the time T_{on} when the switch is closed and the period T. The converter switches between two subtopologies, see Fig. 3.Applying the well-known state-space averaging procedure (see Dixon [2] or Sum [10]) and assuming for a moment that $r_l = r_d = r_s = 0$, we find the following transfer function from the duty cycle to the output voltage:

$$\frac{v_{\mathrm{out}}}{d}(s) = \frac{V_{\mathrm{out}}^2(1-D)^2}{V_{\mathrm{in}}LC} \cdot \frac{\left(1 - \dfrac{LV_{\mathrm{out}}^2}{RV_{\mathrm{in}}^2}s\right)(1 + r_cCs)}{s^2 + \dfrac{(1-D)^2}{RC}s + \dfrac{(1-D)^2}{LC}}. \tag{10}$$

Recall that V_{in}, V_{out}, and D denote fixed values at an operating point, while v_{out} and d denote deviations from this operating point. We see that the above transfer function exhibits an RHPZ z_+ at

$$z_+ = \frac{RV_{\mathrm{in}}^2}{LV_{\mathrm{out}}^2}. \tag{11}$$

If we do not neglect r_l, r_d, and r_s, then the formula of the transfer function discussed above becomes more complicated, of course, but it retains the same features. In our numerical computations, we took these small resistances into account, and for the specific values of this study (see Fig. 2), the audiosusceptibility ($v_{\mathrm{out}}/v_{\mathrm{in}}$), output impedance ($v_{\mathrm{out}}/i_{\mathrm{out}}$), and transfer function from the control input d to the output voltage v_{out} were found to be

$$\mathbf{H}_1(s) = \frac{v_{\mathrm{out}}}{v_{\mathrm{in}}}(s) = \frac{228(s + 45\,460)}{s^2 + 4311s + 5.2 \cdot 10^6} \tag{12}$$

$$\mathbf{H}_2(s) = \frac{v_{\mathrm{out}}}{i_{\mathrm{out}}}(s) = \frac{-0.1(s + 45\,460)(s + 4100)}{s^2 + 4311s + 5.2 \cdot 10^6} \tag{13}$$

$$\mathbf{H}_3(s) = \frac{v_{\mathrm{out}}}{d}(s) = \frac{-0.118(s + 45\,460)(s - 42\,420)}{s^2 + 4311s + 5.2 \cdot 10^6}. \tag{14}$$

The transfer function $\mathbf{H} = [\mathbf{H}_1\ \mathbf{H}_2\ \mathbf{H}_3]$ is our mathematical model for the linearized plant P_0. Note the RHPZ at 42 420 in $\mathbf{H}_3$.

IV. The H^∞ Controller for the Boost Converter

The state-space equations of the averaged and linearized plant P_0 in our design example are

$$\dot{q} = A_0q + B_{1_0}w + B_{2_0}u$$
$$v_{\mathrm{out}} = C_0q + D_{1_0}w + D_{2_0}u$$

where q is the state of the converter (the inductance current and capacitor voltage). The matrices appearing in the state equations are

$$A_0 = \begin{bmatrix} -4208 & -2283 \\ 2086 & -103.1 \end{bmatrix}$$
$$B_{1_0} = \begin{bmatrix} 4975 & 228.3 \\ 0 & -4535 \end{bmatrix}$$
$$B_{2_0} = \begin{bmatrix} 119\,540 \\ -5370 \end{bmatrix}$$
$$C_0 = [0.046 \quad 1]$$
$$D_{1_0} = [0 \quad -0.1]$$
$$D_{2_0} = [-0.118].$$

For our design example, we chose the weight function

$$W(s) = \frac{s + 2\pi \cdot 3500}{s + 2\pi \cdot 500}.$$

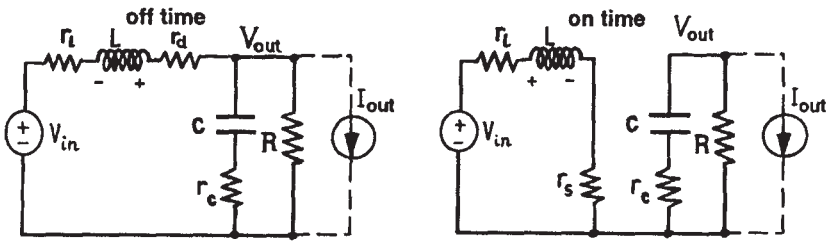

Fig. 3. The two subtopologies of the converter.

By combining P_0 with a realization of W, we obtain the plant $\mathbf{P}$, which is of order three. We must solve the standard problem for $\mathbf{P}$, which is possible, since $\mathbf{P}$ satisfies assumptions (5)–(8). Using the function *hinfopt* of MATLAB to compute the H^∞ controller, we obtain (15), shown at the bottom of the page. The raw controller $\mathbf{C}_0$ has an unstable pole—actually an extremely big positive pole, which cannot be realized by any means. (The closed-loop system would be stable, even if we could realize $\mathbf{C}_0$ and use it.) To overcome this problem, the unstable pole was approximated by a constant

$$\frac{K}{s-a} \sim \frac{-K}{a}, \qquad \text{for } |s| \ll |a|.$$

A similar approximation was used to get rid of the very big zero lying in the right-half plane. Further investigation has shown that these approximations do not affect the performance of the controller over the frequency range of interest (up to about 100 kHz). The approximate H^∞ controller is

$$\mathbf{C}(s) = \left[\frac{-5.56(s+4120)(s+12140)}{(s+3140)(s+45460)} \quad -0.0417\right]. \tag{16}$$

We remark that the H^∞ controller $\mathbf{C}$ has a low dc gain compared to the voltage-mode controller, feedforward controller, or current-mode controller, which will be derived later.

With the controller $\mathbf{C}$, the voltage-attenuation curve looks like that in Fig. 4. In the same figure, the corresponding curves are shown for two other possible choices of the weight function, namely

$$W_1(s) = \frac{s + 2\pi \cdot 350}{s + 2\pi \cdot 50}$$
$$W_2(s) = \frac{s + 2\pi \cdot 35\,000}{s + 2\pi \cdot 5000}.$$

The curves of the output impedance for the three weight functions, when using a logarithmic scale for the impedance, look very similar, so we omit them.

V. Voltage-Mode Control

First, we consider the simple voltage-mode controller of Fig. 5, which measures only the output voltage. (What the controller actually receives is v_{out}, i.e., the difference between the output voltage and a reference voltage.) Applying standard

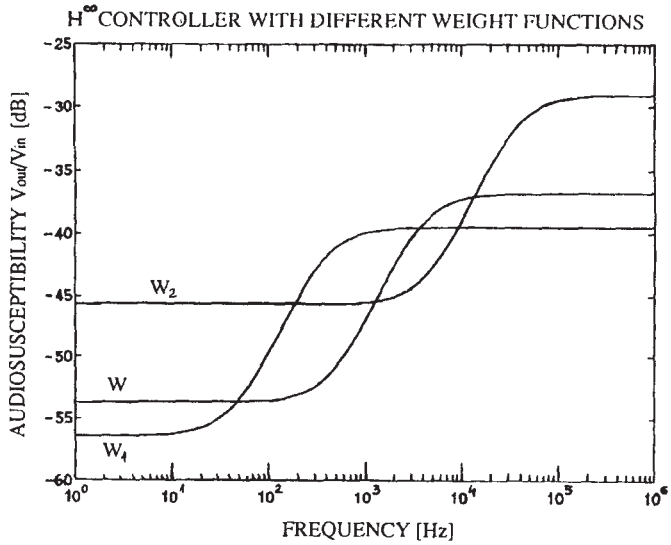

Fig. 4. The input–output voltage-disturbance attenuation with H^∞ controller, with three different weight functions.

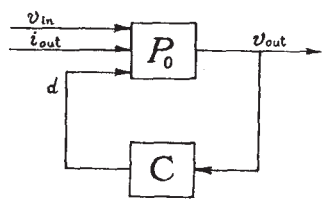

Fig. 5. Block diagram of the converter with voltage-mode control.

design techniques for this controller, see Dixon [2], we obtain its transfer function

$$\mathbf{C}(s) = \frac{-K\left(s + \dfrac{1-D}{3\sqrt{LC}}\right)^2}{s\left(s + \dfrac{1}{r_c C}\right)} = \frac{-3(s+730)^2}{s(s+45\,460)}. \tag{17}$$

This control law was derived following two basic guidelines: 1) to make the low-frequency open-loop gain as large as possible and 2) to obtain a loop gain of less than one at a frequency, which is about half a decade lower than the frequency of the RHPZ.

$$\mathbf{C}_0(s) = \left[\frac{-2.43 \cdot 10^7 (s - 1.02 \cdot 10^8)(s+12140)(s+4120)}{(s - 4.47 \cdot 10^{14})(s+3140)(s+45460)} \quad \frac{1.87 \cdot 10^{13}}{s - 4.47 \cdot 10^{14}}\right]. \tag{15}$$

The expression of the output voltage for the closed-loop system (in terms of Laplace transforms) is

$$v_{\text{out}} = \left[\frac{\mathbf{H}_1}{1-\mathbf{H}_3\mathbf{C}}\right]v_{\text{in}} + \left[\frac{\mathbf{H}_2}{1-\mathbf{H}_3\mathbf{C}}\right]i_{\text{out}}. \tag{18}$$

A more sophisticated version of the voltage-mode controller also includes a feedforward path to reduce the sensitivity of the output voltage to perturbations of the input voltage. The relevant block diagram is again Fig. 1, but without the weight function W. If we denote the components of the controller by $\mathbf{C}_1$ and $\mathbf{C}_2$, then the general expression for the output voltage is

$$v_{\text{out}} = \left[\frac{\mathbf{H}_1+\mathbf{H}_3\mathbf{C}_2}{1-\mathbf{H}_3\mathbf{C}_1}\right]v_{\text{in}} + \left[\frac{\mathbf{H}_2}{1-\mathbf{H}_3\mathbf{C}_1}\right]i_{\text{out}}. \tag{19}$$

From (18) and (19), we see that the feedforward path $\mathbf{C}_2$ can improve the sensitivity from the input voltage to the output voltage, but it cannot improve the output impedance. The stability of the system depends on the feedback part of the controller $\mathbf{C}_1$, so $\mathbf{C}_1$ is chosen as in the voltage-mode control technique discussed earlier, see (17). The static feedforward part of the controller $\mathbf{C}_2$ is chosen to minimize the audio-susceptibility at low frequency, i.e., $\mathbf{H}_1(0)+\mathbf{H}_3(0)\mathbf{C}_2 = 0$, from which

$$\mathbf{C}_2 = -\frac{\mathbf{H}_1(0)}{\mathbf{H}_3(0)}.$$

Consequently, the feedforward controller is

$$\mathbf{C}(s) = \left[\frac{-K\left(s+\dfrac{1-D}{3\sqrt{LC}}\right)^2}{s\left(s+\dfrac{1}{r_cC}\right)} \quad -\frac{\mathbf{H}_1(0)}{\mathbf{H}_3(0)}\right]$$

or expressed numerically

$$\mathbf{C}(s) = \left[\frac{-3(s+730)^2}{s(s+45460)} \quad -0.046\right]. \tag{20}$$

VI. Current-Mode Control

The current-mode controller includes both voltage and current-feedback loops. The inductor current I_L is being measured and fed to the so-called inner-loop controller. The latter helps stabilize the system by transforming the two complex poles of the power stage into two real poles. One of them is close to the origin, and the other has a high corner frequency, see Dixon [2] or Pressman [8]. To prevent subharmonic oscillations at a duty cycle $D > 0.5$, a slope-compensation scheme is applied. In this case, the duty cycle can be expressed as

$$D = \frac{(V_c - I_L K_s) f_s L}{LM_c + 0.5K_sV_{\text{in}}} \tag{21}$$

where f_s is the switching frequency, M_c is the compensation slope, and K_s is the inner current-loop gain, see Middlebrook [7]. It should be noted that (21) is an approximation valid for the small-signal analysis considered here. For large-signal transients, one should apply the more accurate formula of Verghese *et al.* [11], see also Kimhi and Ben-Yaakov [5].

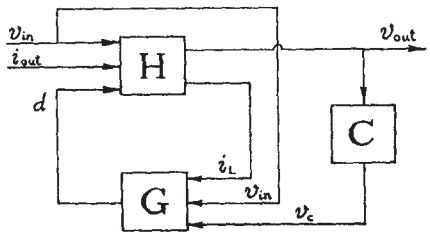

Fig. 6. Block diagram of the converter with current-mode control.

Describing the current-mode controller by the generic model of Fig. 6, we can use (21) to derive the components of the linearized inner-loop controller G:

$$\mathbf{G}_1 = \frac{\partial d}{\partial i_L} = \frac{-f_sK_sL}{LM_c + 0.5K_sV_{\text{in}}}$$

$$\mathbf{G}_2 = \frac{\partial d}{\partial v_{\text{in}}} = \frac{-K_sf_sL(V_C - I_L)}{(LM_c + 0.5K_sV_{\text{in}})^2}$$

$$\mathbf{G}_3 = \frac{\partial d}{\partial v_c} = \frac{f_sL}{LM_c + 0.5K_sV_{\text{in}}}.$$

We denote by $\mathbf{H}_1, \cdots, \mathbf{H}_6$ the components of the transfer function of the power stage

$$\mathbf{H} = \begin{bmatrix}\mathbf{H}_1 & \mathbf{H}_2 & \mathbf{H}_3\\ \mathbf{H}_4 & \mathbf{H}_5 & \mathbf{H}_6\end{bmatrix}.$$

Here, $\mathbf{H}_1$, $\mathbf{H}_2$, and $\mathbf{H}_3$ are the same as in (12)–(14). Using the controller G, we have (in terms of Laplace transforms)

$$v_{\text{out}} = \left[\mathbf{H}_1 + \frac{\mathbf{H}_3(\mathbf{G}_1\mathbf{H}_4 + \mathbf{G}_2)}{1-\mathbf{G}_1\mathbf{H}_6}\right]v_{\text{in}} + \left[\mathbf{H}_2 + \frac{\mathbf{H}_3\mathbf{G}_1\mathbf{H}_5}{1-\mathbf{G}_1\mathbf{H}_6}\right]i_{\text{out}} + \frac{\mathbf{H}_3\mathbf{G}_3}{1-\mathbf{G}_1\mathbf{H}_6}v_c$$

where the transfer function from v_c to v_{out} (without C) is

$$\frac{v_{\text{out}}}{v_c} = \frac{\mathbf{H}_3\mathbf{G}_3}{1-\mathbf{G}_1\mathbf{H}_6}.$$

The numerical values for the present case are

$$\frac{v_{\text{out}}}{v_c}(s) = \frac{-0.194(s+45460)(s-42240)}{(s+210)(s+613550)} \tag{22}$$

The current feedback does not influence the RHPZ, but it splits the complex poles into two real poles. Formula (22) was used to design the outer-loop controller C, which is the voltage feedback part. We obtained

$$\mathbf{C}(s) = \frac{10^6(s+210)}{s(s+45460)} \tag{23}$$

VII. Simulation and Experimental Results

The performance of the closed-loop system with the four controllers described above [(16), (17), (20), and (23)] has been examined by HSPICE simulation, time domain, and frequency domain. To be consistent, the same controller structure, using three operational amplifiers, was used throughout. The same controller configuration was used also in the laboratory

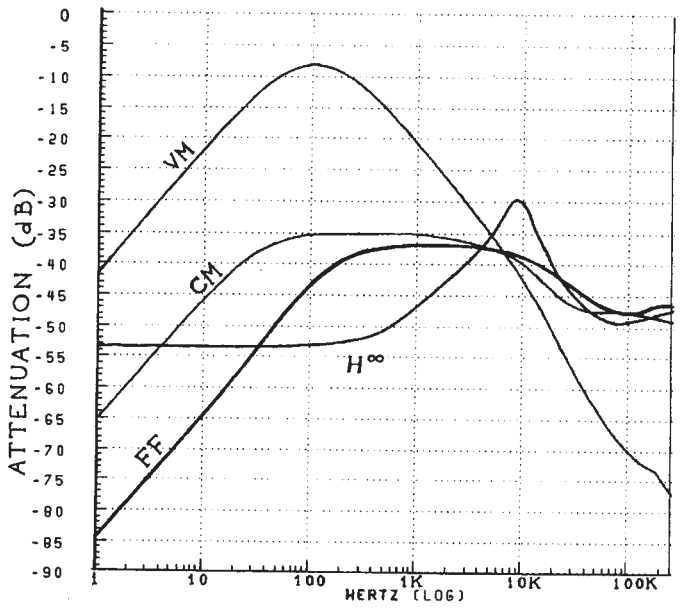

Fig. 7. The input–output voltage-disturbance attenuation in decibels.

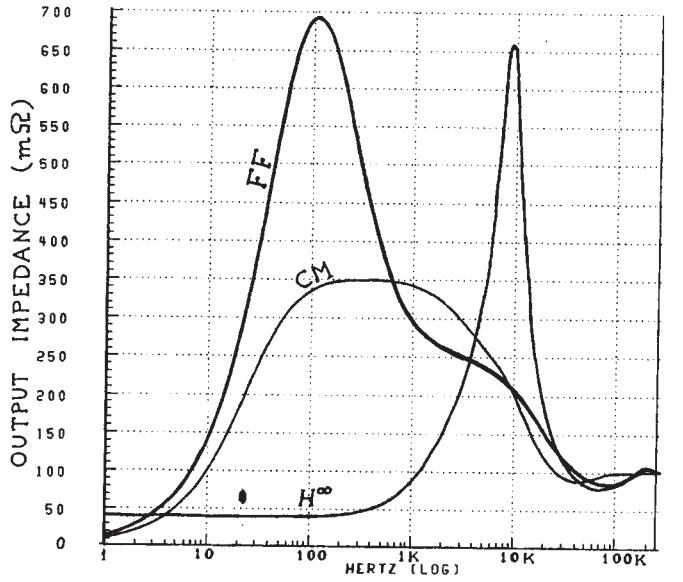

Fig. 8. The output impedance in mΩ.

experiments. The simulation took into account the actual response of the commercial amplifiers of type MC3314. The power stage was represented using an Average Switched Inductor Model of Ben-Yaakov [1]. In Figs. 7 and 8, the voltage-disturbance attenuation and output impedance of the closed-loop systems are shown for the four different controllers mentioned above according to the simulation. The plots are marked voltage-mode control (VM), current-mode control (CM), feedforward control (FF), and H^∞ control (H^∞).

We see that at very low frequencies, the H^∞ controller is not as good as the others, but it maintains practically constant performance levels up to about 1 kHz, and it outperforms the other controllers between 10 Hz and 3 kHz, especially with regard to output impedance.

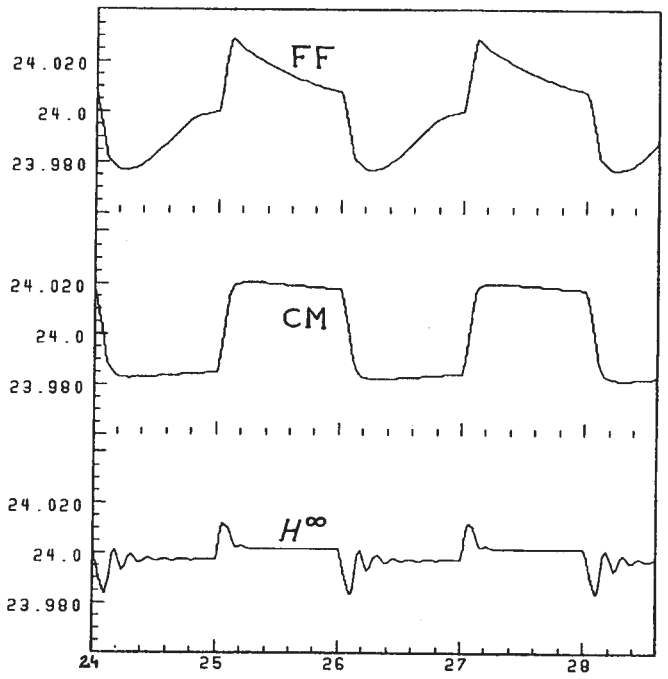

Fig. 9. The output voltage with rectangular perturbation in the input voltage, ±1 V.

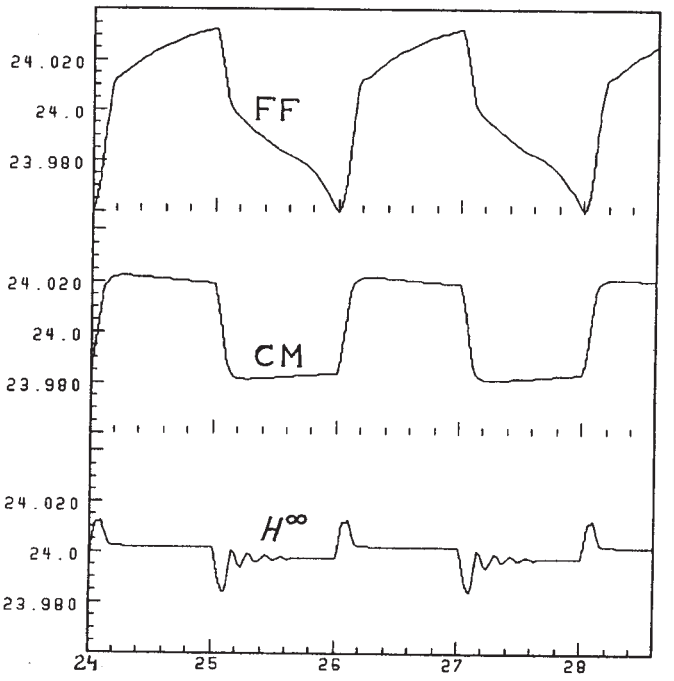

Fig. 10. The output voltage with rectangular perturbation in the load, ±50 mA.

Fig. 9 shows the steady-state output voltage of the closed-loop system, with the different controllers, when a square-wave input-voltage disturbance of ±1 V is added to the nominal input voltage of 12 V at 500 Hz. The curves are marked CM, FF, and H^∞ as before. The voltage-mode control is not shown because it performs much worse than the others. The time runs from 22 to 30 ms, measured from the moment when the circuit was turned on.

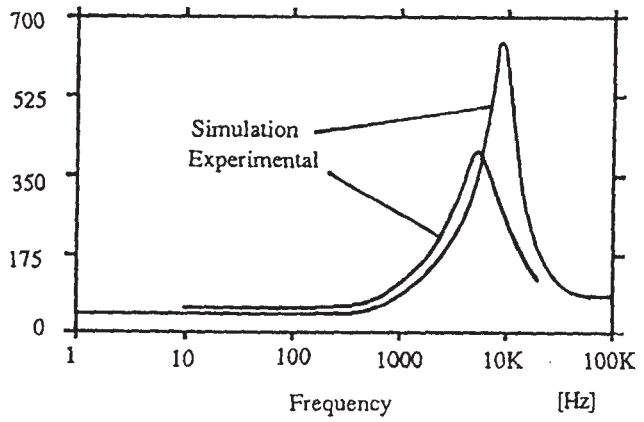

Fig. 11. Simulation and experimental results of output impedance of H^∞ controlled boost converter.

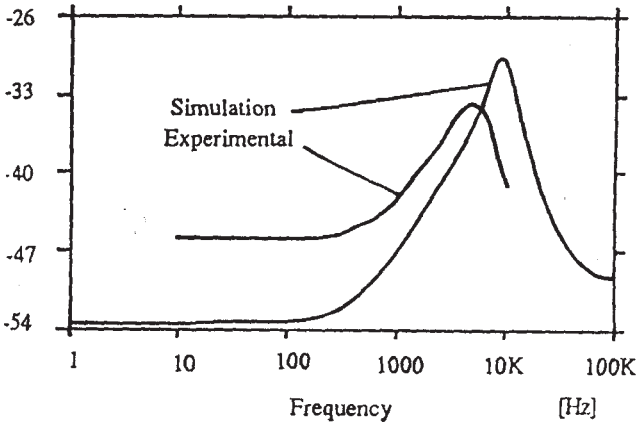

Fig. 12. Simulation and experimental results of audiosusceptibility of H^∞ controlled boost converter.

Fig. 10 is similar, but now the disturbance is added to the output current, and it is ±50 mA (over the nominal 0.5 A). Again, the voltage-mode control is not shown because the curve overlaps with that of the feedforward control.

The H^∞ controller studied in the simulations has also been realized and tested in the laboratory. The simulation results were found to be in good agreement with the experimental results, as can be seen in Figs. 11 and 12.

REFERENCES

[1] S. Ben-Yaakov, "SPICE simulation of PWM DC–DC converter systems: Voltage feedback, continuous inductor conduction mode," *IEEE Electron. Lett.*, vol. 25, no. 16, pp. 1061–1062, 1989.

[2] L. H. Dixon, "Closing the feedback loop," in *Switching Regulated Power Supply Design Seminar Manual.* Lexington, KY: Unitrode, 1986.

[3] J. C. Doyle, K. Glover, P. P. Khargonekar, and B. A. Francis, "State space solutions to standard H_2 and H_∞ control problems," *IEEE Trans. Automat. Contr.*, vol. 34, no. 8, pp. 831–847, 1989.

[4] B. A. Francis, *A Course in H_∞ Control Theory.* New York: Springer-Verlag, 1987.

[5] D. Kimhi and S. Ben-Yaakov, "A SPICE model for current mode PWM converters operating under continuous inductor current conditions," *IEEE Trans. Power Electron.*, vol. 6, no. 2, pp. 281–286, 1991.

[6] D. Limebeer and M. Green, *Linear Robust Control.* Englewood Cliffs, NJ: Prentice-Hall, 1995.

[7] R. D. Middlebrook, "Topics in multiple-loop regulators and current-mode programming," in *IEEE Power Electronics Specialists Conf. Rec.*, 1985, pp. 716–732.

[8] A. Pressman, *Switching Power Supply Design.* New York: McGraw-Hill, 1991.

[9] M. G. Safonov, D. J. N. Limebeer, and R. Y. Chiang, "Simplifying the H_∞ theory via loop shifting, matrix pencil and descriptor concepts," *Int. J. Control*, vol. 50, no. 6, pp. 2467–2488, 1989.

[10] K. K. Sum, *Switch Mode Power Conversion.* New York: Marcell Dekker, 1989.

[11] G. C. Verghese, C. A. Bruzos, and K. N. Mahabir, "Averaged and sampled-data models for current mode control: A reexamination," in *IEEE Power Electronics Specialists Conf. Rec.*, 1989, pp. 484–491.

Rami Naim was born in Teheran, Iran, in 1965. He received the B.Sc. degree in electrical engineering from the Technion, Haifa, Israel, in 1990 and the M.Sc. degree from Ben-Gurion University, Beer Sheva, Israel, in 1994.

His interests are in modeling and analysis of control systems, especially applied to switch-mode power supplies. Presently, he works in the Power Systems Group at the TELRAD Telecommunications Company, Lod, Israel.

George Weiss received the control engineering degree from the Polytechnic Institute of Bucharest, Romania, in 1981 and the Ph.D. degree in applied mathematics from Weizmann Institute, Rehovot, Israel, in 1989.

He worked at Ben-Gurion University, Beer Sheva, Israel, and is now at the School of Engineering, University of Exeter, Exeter, U.K. His research interests include distributed parameter systems, operator semigroups, optimal and robust control, sampling theory, and power electronics.

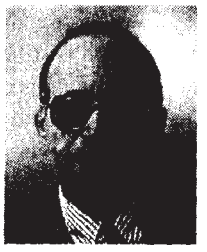

Shmuel (Sam) Ben-Yaakov received the B.Sc. degree from the Technion, Haifa, Israel, in 1961 and the M.S. and Ph.D. degrees from the School of Engineering, University of California, Los Angeles, in 1967 and 1970, respectively.

He is a Professor at the Department of Electrical and Computer Engineering, Ben-Gurion University, Beer Sheva, Israel, and heads the Power Electronics Group there. He is involved in research, design, and development of switch-mode and resonant systems in both the academic and industrial environments. He serves as a consultant to commercial companies on analog circuit design and power-electronics-related issues.